Published in final edited form as:

Neurogenetics. 2007 April ; 8(2): 121–130. doi:10.1007/s10048-006-0078-5.

Nf1 expression is dependent on strain background: implications for tumor suppressor haploinsufficiency studies

Jessica J. Hawes,

Mouse Cancer Genetics Program, National Cancer Institute-Frederick, West 7th Street at Fort Detrick, P.O. Box B, Building 560, Rm 31-20, Frederick, MD 21702, USA

Robert G. Tuskan,

Mouse Cancer Genetics Program, National Cancer Institute-Frederick, West 7th Street at Fort Detrick, P.O. Box B, Building 560, Rm 31-20, Frederick, MD 21702, USA

Karlyne M. Reilly

Mouse Cancer Genetics Program, National Cancer Institute-Frederick, West 7th Street at Fort Detrick, P.O. Box B, Building 560, Rm 31-32B, Frederick, MD 21702, USA

Abstract

Neurofibromatosis type 1 (NF1) is the most common cancer predisposition syndrome affecting the nervous system, with elevated risk for both astrocytoma and peripheral nerve sheath tumors. NF1 is caused by a germline mutation in the *NF1* gene, with tumors showing loss of the wild type copy of *NF1*. In addition, NF1 heterozygosity in surrounding stroma is important for tumor formation, suggesting an additional role of haploinsufficiency for *NF1*. Studies in mouse models and NF1 families have implicated modifier genes unlinked to *NF1* in the severity of the disease and in susceptibility to astrocytoma and peripheral nerve sheath tumors. To determine if differences in *Nf1* expression may contribute to the strain-specific effects on tumor predisposition, we examined the levels of *Nf1* gene expression in mouse strains with differences in tumor susceptibility using quantitative polymerase chain reaction. The data presented in this paper demonstrate that strain background has as much effect on *Nf1* expression levels as mutation of one *Nf1* allele, indicating that studies of haploinsufficiency must be carefully interpreted with respect to strain background. Because expression levels do not correlate entirely with the susceptibility or resistance to tumors observed in the strain, these data suggest that either variation in *Nf1* levels is not responsible for the differences in astrocytoma and peripheral nerve sheath tumor susceptibility in *Nf1*−/+;*Trp53*−/+*cis* mice, or that certain mouse strains have evolved compensatory mechanisms for differences in *Nf1* expression.

Keywords

Neurofibromatosis; *Nf1*; Haploinsufficiency; Astrocytoma; Peripheral nerve sheath tumor

kreilly@ncifcrf.gov.

Introduction

Neurofibromatosis type 1 (NF1) is an autosomal dominant tumor suppressor syndrome predisposing individuals to develop multiple tumors of the central and peripheral nervous system, such as astrocytomas, glioblastomas [1], malignant peripheral nerve sheath tumors, and neurofibromas [2, 3]. This familial cancer syndrome results from inheritance of inactivating mutations in the *NF1* gene and affects as many as 1 in 3,500 people.

The tumor suppressor neurofibromin is the protein product of the *NF1* gene. Neurofibromin is a GTP-ase activating protein that functions as a tumor suppressor by negatively regulating the activation of the proto-oncogene p21-ras and downstream mitogenesis [4-7]. *Nf1*-deficient cells are associated with elevated p21-ras activity and increased cellular proliferation. Thus, neurofibromin negatively regulates cellular proliferation, and loss thereof leads to over-activation of the ras pathway and proliferation. Studies with mice heterozygous for *Nf1* suggest that neurofibromin may also be upstream of other signaling pathways and cellular processes [8-13]. For example, mast cells heterozygous for *Nf1* secrete elevated levels of TGF-beta [12], and in some bone tissues, the neurofibromin–ras pathway may cross-talk with the protein kinase A pathway to regulate gene expression [13]. There is also evidence supporting a role for neurofibromin in wound healing, fibroblast proliferation, and collagen deposition [14].

Knockout studies have shown that *Nf1* is an essential gene. *Nf1* knockout mice are embryonic lethal with an abnormal cardiac development phenotype [15]. Mice specifically lacking *Nf1* in the CNS result in an increase in proliferation of glial progenitor cells that leads to optic gliomas [16]. Spinal cords from *Nf1* −/− embryos have an increased number of oligodendrocyte progenitor cells [17], and *Nf1* −/− neural stem cells (NSC) exhibit a growth and survival advantage over wild type (WT) NSCs [18]. Furthermore, mice heterozygous for *Nf1* have a predisposition for various tumors including those seen in NF1 patients, such as pheochromocytoma [19, 20] and myeloid leukemia [15]. These data suggest that the *Nf1* gene is essential for proper cardiac and CNS development, and loss thereof predisposes mice to tumor development.

Nf1 haploinsufficiency in a variety of cells in the tumor microenvironment can also play an important role in tumorigenesis by affecting several different cellular processes [10]. *Nf1* haploinsufficiency was reported to modulate melanocyte and mast cell fates [8], and Nf1 heterozygous (+/−) mast cells were shown by several groups to play an important role in neurofibroma formation [8, 12, 13]. *Nf1* +/− mast cells were also shown to have increased variation in dendrite formation [9]. Astrocytes heterozygous for *Nf1* show decreased cell attachment and increased motility [21] as well as a growth advantage [22]. Other data suggests that *Nf1* +/− endothelial cells, and possibly inflammatory cells, augment angiogenesis [11]. As *Nf1* heterozygosity has been shown to modulate multiple biological processes related to tumor formation, this suggests that tumor susceptibility may be sensitive to relatively small changes in *Nf1* expression, such as changes in gene dosage in haploinsufficient cells. Therefore, events that mediate changes in *Nf1* expression levels may also play an important role in tumor susceptibility.

Despite the importance of *Nf1* expression levels in multiple processes, levels of *Nf1* expression are not likely to be consistent throughout the population. Microarray data available online from the GeneNetwork database [23] suggest that some mouse strains have differing levels of *Nf1* expression. As *Nf1* expression levels play an important role in tumorgenicity, we hypothesized that variation in *Nf1* expression levels in the population may affect tumor susceptibility.

Mice carrying mutant copies of both *Trp53* and *Nf1* on the same chromosome (*NPcis*) have been developed by several groups as a model to study NF1 [24-27]. *TP53* in human and *Trp53* in mice encode the tumor suppressor p53 protein, which serves as a key component of the cell-cycle checkpoint by responding to DNA damage and cellular stress and by acting as a transcription factor to turn on genes responsible for growth arrest and apoptosis. *Nf1* and *Trp53* are closely linked on mouse chromosome 11 and can be lost together in a single genetic event during loss of heterozygosity in *NPcis* mice, resulting in the development of aggressive astrocytoma and genetically engineered murine peripheral nerve sheath tumors (GEM PNST), among other tumor types. Tumor susceptibility is dependent on the background strain carrying the *NPcis* mutations, with *NPcis* mice on the C57BL/6J (B6) background strain developing astrocytoma with high penetrance and *NPcis* mice on the 129S4/SvJae (129) background strain being resistant to astrocytoma [25, 26]. Conversely, *NPcis* mice on either the B6 or the 129 backgrounds are susceptible to GEM PNST development. However, crossing the B6 strain to the A/J strain results in *NPcis* F1 progeny that are resistant GEM PNSTs but susceptible to astrocytoma [28]. As different background strains have different susceptibilities to tumor development and tumorgenicity may be sensitive to *Nf1* expression levels, we examined *Nf1* in tumor-prone tissues on different strain backgrounds to determine if *Nf1* expression levels are linked to tumor susceptibility.

Results

Microarray data available online at http://www.genenetwork. org was used to examine variation in *Nf1* expression in the brain and whether or not the genomic regions controlling *Nf1* expression overlapped with the genomic regions previously identified as important for susceptibility to NF1-associated tumorigenesis. Two datasets were examined. In the first dataset generated by R.W. Williams et al. at the University of Tennessee and University of Memphis, mRNA expression in adult midbrain and forebrain from B6, DBA/2J, F1 hybrids, and 42 B×D recombinant inbred lines was examined using Affymetrix M430A and B arrays. In the second dataset generated by G.D. Rosen et al. at Beth Israel Deaconess Medical Center, mRNA expression in adult striatum from B6, DBA/2J, and 31 B×D recombinant inbred lines was examined using Affymetrix M430v2 arrays. In both cases, variation in *Nf1* gene expression was seen between different B×D recombinant inbred strains. Interval mapping was used in the WebQTL program to find regions of the genome that showed linkage to the variation in *Nf1* expression in different B×D strains. One of the linkage peaks identified in the striatum data overlapped with the *Nstr2* locus we have identified as a modifier of GEM PNSTs (Fig. 1a) [28]. One of the linkage peaks identified in the midbrain and forebrain data overlapped with the *Nstr1* locus (Fig. 1b). This analysis suggested that control of *Nf1* expression is cell-type specific and that genomic regions controlling *Nf1* expression may also control tumor susceptibility. To address these possibilities, we used

quantitative polymerase chain reaction (qPCR) to examine levels of *Nf1* mRNA in precursor tissues for NF1-associated tumors.

Two sets of primers specifically amplifying *Nf1* cDNA were characterized for use in *Nf1* expression studies by qPCR. For primer set number 1, the forward primer binds within exon 53, and the reverse primer binds within exon 55 of the *Nf1* gene (accession number NM_010897). The genomic region between these primers spans two introns and 3.3 kb of genomic DNA. However, there are only 332 base pairs (bp) of mRNA or cDNA in between these primers. Both primers have no predicted hairpins, dimers or cross-dimers, and perfect primer ratings of 100 when analyzed by NetPrimer (http://www.premierbiosoft.com/netprimer/netprlaunch/netprlaunch.html). Standard polymerase chain reaction (PCR) using an annealing temperature gradient from 50 to 70°C was used to identify the ideal annealing temperature, to verify the PCR product size, and to verify amplification of a single product (Fig. 2a). The use of any annealing temperature between 50 and 70°C results in a single PCR product of the correct anticipated size of 332 bp amplified from WT 129 brain cDNA templates. These data suggest that *Nf1* primer set number 1 specifically amplifies *Nf1* cDNA derived from mRNA transcribed from exons 54 through 56.

The second set of primers bind within exons 57 and 58, targeting the last two exons of the *Nf1* gene. These two primers span 8 kb of genomic DNA and an expected 244 bp of mRNA/cDNA. Both the forward and reverse primers of primer set number 2 also have perfect primer ratings of 100 and no predicted hairpins, dimmers, or crossdimers when analyzed by NetPrimer. These primers amplify a single band of 244 bp from WT 129 brain cDNA templates at annealing temperatures 50 to 60°C (Fig. 2b). These data suggest that the *Nf1* primer set number 2 specifically amplifies full-length *Nf1* cDNA transcribed from exons 58 through 59. Both primers were used to confirm all experimental results, although only the data from one representative reaction is shown.

Although the correct product size could only be theoretically amplified from mRNA transcribed into cDNA and not from genomic DNA, controls were used to verify the lack of genomic DNA contamination in cDNA templates. Control cDNA templates were made in absence of reverse transcriptase (RT) enzyme in the RT reaction and alongside WT samples. Standard PCR using *Nf1* primer set number 1 results in no PCR product visible in no-RT controls (Fig. 3a). These data confirm that there is no genomic DNA contaminating the RNA preparations and that the PCR product is generated purely from mRNA reverse transcribed into cDNA.

To further verify the specificity of the primer sets for *Nf1* cDNA, *Nf1* knockout (−/−) embryos were obtained and analyzed for expression of *Nf1*. Embryos were isolated at embryo day 13.5 post coitum and washed and divided into segments for isolation of DNA or RNA. Genotyping was used to identify knockout (−/−) embryos from heterozygous (+/−) and WT (+/+) littermates (Fig. 3b). qPCR using embryo cDNA templates results in the absence of *Nf1* qPCR product in −/− templates, despite the presence of product from the β-tubulin internal control reaction (Fig. 3c). Furthermore, qPCR results are similar to standard PCR results, in that the reaction results in a single product visualized by separation on an agarose gel (Fig. 3c) and a single dissociation peak (Fig. 3d). These data further show that

both *Nf1* primer sets specifically amplify cDNA from *Nf1* mRNA and reflect *Nf1* expression in whole tissues.

To determine if the two *Nf1* primer sets are sensitive enough to reflect changes in levels of *Nf1* expression, serial dilutions of WT cDNA templates were analyzed by qPCR (Fig. 4). Serial dilutions result in consistent increases in the number of cycles required for product formation to reach threshold (Ct; Fig. 4a,c). Furthermore, the increase in Ct is linear with respect to the template dilutions, as seen by regression values (R^2) ≥ 0.95 (Fig. 4b,d). These data suggest that differences in *Nf1* expression levels can be quantitatively detected in cDNA templates using both *Nf1* primer sets.

The *Nf1* Exon 9a isoform is a brain-specific, alternatively spliced full-length *Nf1* isoform that is conserved in the mouse and contains 30 additional nucleotides at the C-ermini of exon 9 [29]. Because the *Nf1* primer sets described above do not distinguish between these two full-length *Nf1* isoforms, we designed primers to specifically amplify the *Nf1* exon 9a isoform to determine if the pattern of expression differs from that obtained with the C-terminal *Nf1* primers described above. Two distinct primer sets targeting the region of exon 9a were similarly characterized as before (data not shown). The increase in Ct for the *Nf1* exon 9a isoform is also linear with respect to the template dilution (Fig. 4f). These data suggest that differences in the *Nf1* exon 9a isoform expression levels can also be quantitatively detected by qPCR.

As *NPcis* mice are susceptible to spontaneous tumor formation and are heterozygous for WT *Nf1*, qPCR was used to determine if *NPcis* mice have decreased *Nf1* expression or if there is compensation to maintain normal levels of expression despite the loss of one WT allele. Messenger RNA from the brains of WT and *NPcis* mice on three different background strains were simultaneously reverse transcribed into cDNA and analyzed for *Nf1* expression by qPCR using both *Nf1* C-terminal and *Nf1* exon 9a primer sets (Fig. 5a,b). *NPcis* mice on all three backgrounds express significantly less *Nf1* as compared to WT animals on the same background using the C-terminal primers. In addition, *Nf1* expression is significantly higher in the brains of mice on the B6 strain as compared to 129 mice (Figs. 5 and 6a). Furthermore, the magnitude of the change in *Nf1* expression levels seen in *NPcis* mice as compared to WT (e.g., 100 vs 66% for B6) is similar to the magnitude of the change seen between the B6 and 129 background strains (100 vs 70%). These data are also very similar to the trend in expression levels of *Nf1* exon 9a (Fig. 5b), which showed somewhat greater variability than the C-terminal primer sets. These data suggest that *NPcis* mice on all three backgrounds are haploinsufficient for *Nf1* and that the degree of *Nf1* haploinsufficiency is equivalent to the degree of difference between the B6 and 129 strains.

NPcis mice on the B6 background, as well as *NPcis* F1 progeny from B6 and AJ crosses (B6×A), and F1 progeny from B6 and DBA/2J (DBA; B6×DBA) crosses are susceptible to astrocytoma formation, whereas *NPcis* mice on the 129 background are resistant to astrocytoma. Therefore, *Nf1* expression levels in the brains of mice from the background strains B6, 129, B6×A, and DBA were compared by qPCR analysis to determine if differences in *Nf1* expression levels correlate with astrocytoma susceptibility. Expression levels of *Nf1* were also compared among several other inbred background strains to

determine if variation in *Nf1* expression extends to other background strains. B×D recombinant inbred strains were chosen based on expression data available on GeneNetwork that showed variation in *Nf1* expression in the brain. In the midbrain and forebrain dataset, B×D39/TyJ (B×D39) was one of the lowest expressers, whereas B×D40/TyJ (B×D40) was the highest expresser. B×D38/TyJ (B×D38) was chosen as a mid-level expresser. Although *Nf1* expression is significantly higher in the brains of mice on the B6 strain as compared to 129 mice (Figs. 5 and 6a), similar levels of *Nf1* expression were seen in the brains of B6, B6×A, inbred DBA, and recombinant inbred B×D38, B×D39, and B×D40 mice. These data suggest that the brains of the 129 mice that are resistant to astrocytoma express *less* of the tumor suppressor *Nf1* than the brains of other strain backgrounds.

Levels of *Nf1* expression in the sciatic nerve of the different background strains were also compared to determine if *Nf1* expression levels correlate with background susceptibility to GEM PNSTs (Fig. 6b). In the case of GEM PNST susceptibility, *NPcis* mice on a B6 background or a 129 background are susceptible, whereas *NPcis* mice on a B6×A or B6×DBA F1 background are resistant. As in the brain, *Nf1* expression levels in the sciatic nerve were significantly decreased in the 129 strain as compared to B6. On the other hand, the *Nf1* expression level in the B6 strain is similar to those in the B6×A and DBA strains. These data suggest that differences in *Nf1* expression levels do not correlate with differences in strain susceptibility to GEM PNSTs. The recombinant strains B×D38, B×D39, and B×D40 exhibit a trend for higher levels of *Nf1* expression than the other background strains, further suggesting that *Nf1* expression is variable among different background strains and between different tissues within the strain.

Materials and methods

Bioinformatics

The GeneNetwork (http://www.genenetwork.org/search.html) was searched for *Nf1* in mouse B×D datasets from the brain. Specifically, the INIA Brain mRNA M430 (April 2005) PDNN dataset of mid- and forebrain expression arrays and the HBP/Rosen Striatum M430v2 (April 2005) PDNN of striatum expression arrays were examined. Probe sets were verified for their binding to the *Nf1* mRNA using a blast-like alignment tool (BLAT) search in the UCSC Genome Browser that is linked to GeneNetwork. The Affy array probes 1452525_a_at_A and 1438067_at_A were chosen as validated probes for *Nf1*. WebQTL interval mapping was used to determine regions of the genome responsible for variation in *Nf1* expression levels across different B×D strains. Permutation tests with 1,000 replicates were used in the WebQTL program to determine the statistical significance of the mapping, with the significance threshold set to P=0.05 and a suggestive threshold set to P=0.63. Bootstrap sampling by WebQTL was also used to confirm the best location of the linkage peaks.

cDNA Templates

All samples were derived from female mice between 2 and 3 months of age. All mice were bred and maintained at the National Cancer Institute (NCI)-Frederick according to the guidelines and regulations of the Animal Care and Use Committee. *NPcis* mice on the

C57BL/6J background were backcrossed greater than 20 generations. *NPcis* mice on the 129S4/SvJae background were maintained as inbred from the time of generating the mutant *Nf1* and *Trp53* allele. Brain samples include the forebrain and midbrain minus the olfactory bulb. Brains and sciatic nerves were immediately frozen on dry ice after dissection and stored at −80°C. A dounce homogenizer was used to homogenize brain tissue, and a grinder was used to homogenize sciatic nerve tissues. Total RNA was extracted with TRIZOL according to manufacturer's instructions. An amount of 10 μg RNA was treated with DNase (DNA-free, Ambion) and repurified using the Qiagen RNEasy kit. RNA samples were normalized to 100 ng/ml (±5 ng/ml) for brain or 75 ng/ml (±5 ng/ml) for sciatic nerve. An amount of 50 ng of total mRNA was reverse transcribed into Cdna using oligo dT primers and the SuperScript III First-strand synthesis system (Invitrogen) according to manufacturer's instructions. A volume of 1 μl of cDNA from each reverse transcriptase reaction was used as template for PCR experiments.

Primers

The sequence for the *Nf1* primer set number 1 forward primer is 5′-CGCAGCAGCACCCACATTTAC-3′,and the sequence of the reverse primer is 5′-ACTGTGGCGGGGACTCCTCA-3′. The sequence for the *Nf1* primer set number 2 forward primer is 5′-TTCTTGATGCCTTGATTGAC-3′, and the sequence of the reverse primer is 5′-CACTTGGCTTGCGGAT. The sequence for the *Nf1* exon 9a primer set number 1 forward primer is 5′-ACGAGAGCAACATAAACAAGAAG-3′, and the sequence of the reverse primer is 5′-AGAAGCAGTGC CAAGTCCAT-3′. The sequence for the *Nf1* exon 9a primer set number 2 (data not shown) forward primer is 5′-TTGTGTCAAGTTGTGTAAAGC-3′, and the sequence of the reverse primer is 5′-AGAAGCAGTGCCAAGTCCAT-3′. The forward (5′-CCGGGGCAGCCAACAGTACC-3′) and reverse (5′-CTCGGGGCGGGATGTCACAC-3′) β-tubulin primers used as internal controls have been previously described elsewhere [30]. Primers and PCR fragments were checked for the presence of SNPs between the B6 and 129 strains in the current Mouse Genome Build 36, and no SNPs were found.

Standard PCR

ThermalAce DNA polymerase (Invitrogen) was used in all standard PCR reactions. Annealing temperature gradients between 50 and 70°C were used to determine the ideal annealing temperature for each primer set. PCR products were separated on 2% agarose/1×TAE DNA gels.

Quantitative PCR

Brilliant SYBR Green (Stratagene), master mix or core kit, was used for each qPCR reaction. A volume of 1 μl of each cDNA template was assayed in duplicate alongside an internal control (β-tubulin), also in duplicate. PCR products were analyzed for the number of cycles required to reach the threshold using a quantitative real-time PCR machine, the MX4000 (Stratagene). MX4000 software was used to calculate the relative amount of each product compared to internal β-tubulin controls and a standard calibrator. All data were calculated as percent (%) control of the average WT C57BL/6 values. Significance was determined using repeated-measures analysis of variance (ANOVA) and Tukey's HSD post

hoc test [31] (http://www.graphpad.com/articles/library.cfm) with $P<0.05$ considered to be significant.

Nf1 knockout embryos

Heterozygous *Nf1* mice were bred to generate litters of WT, heterozygous, and knockout embryos. On embryonic day 13.5, pregnant female mice were euthanized by CO_2 asphyxiation, and the embryos were rapidly removed and placed in sterile phosphate-buffered saline (PBS). Embryos were removed and washed three times for 5 min in fresh PBS. Embryos were then sectioned for DNA or RNA extraction and frozen on dry ice. Breeding of mice and isolation of embryos were performed according to the guidelines and regulations of the NCI-Frederick Animal Care and Use Committee.

Conclusions

A bioinformatics approach, using publicly available datasets of brain expression levels, was used to generate a hypothesis that modifiers of nervous system tumorigenesis control levels of *Nf1* expression. We compared the loci responsible for variation in *Nf1* expression to the loci modifying GEM PNST tumorigenesis and found that, in particular datasets, control of *Nf1* expression overlapped the modifier loci, *Nstr1* and *Nstr2*. To test our hypothesis, we have developed two sets of quantitative PCR primers to *Nf1* to look at levels of *Nf1* expression in the nervous system of strains susceptible and resistant to nervous system tumors.

Two different primer sets annealing to the final 3′ exons of the *Nf1* gene were thoroughly characterized and shown to specifically and quantitatively amplify *Nf1* transcript by standard PCR and qPCR. Both sets of primers are also very sensitive to changes in expression levels, detecting an almost 50% decrease in *Nf1* expression in *Nf1* heterozygous animals. The decrease in *Nf1* expression further suggests that the amount of *Nf1* expression lost by losing one WT *Nf1* allele is not compensated for by other mechanisms at the transcriptional level.

Although many splice isoforms of *NF1* have been identified in humans [29, 32, 33], only the brain-specific exon 9a isoform has been shown to be conserved in mice [29]. We, therefore, developed two different primer sets to specifically amplify the exon 9a isoform of *Nf1*. Although the amplification of exon 9a using these primers was more variable than amplification of the C-terminal, as evidenced by greater variability in replicates, the same trends were observed for exon 9a as were seen for the C-terminus in the brain. This suggests that the strain-specific control of *Nf1* expression is not isoform-specific.

In the brain, we found that the level of *Nf1* expression may loosely correlate to susceptibility to astrocytoma, with the resistant strain, 129, showing lower levels of *Nf1* expression than the susceptible strains. This result was counter to our expectation that resistant strains might have higher basal levels of the tumor suppressor *Nf1* and, therefore, be more protected from tumorigenesis. Because neurofibromin, the product of the *Nf1* gene, acts as a rasGAP protein to downregulate ras activity, this result may be explained by compensating increases in RasGEF pathways in susceptible strains to keep ras regulation in balance within the

susceptible strains. When *Nf1* is lost at the initiation of tumorigenesis, these cells may experience a higher basal level of ras activity. Using the GeneNetwork Association Network function (http://www.genenetwork.org), we checked whether any RasGEFs showed strong negative correlation to the level of *Nf1* gene expression in the datasets we used for our original hypothesis on variation of *Nf1* expression levels. We found weak negative correlation of *Nf1* expression levels and the levels of *Rasgef1b, Rasgef1c*, and *Rasgrp1* in the INIA Brain mRNA M430 dataset (see Materials and methods) and weak correlation of *Nf1* expression levels and *Rasgrf1* and *Rasgef1a* in the HBP/Rosen Striatum M430v2 dataset. We successfully designed primers for qPCR for *Rasgef1b* and *Rasgef1c* but found no statistically significant differences in the levels of these RasGEFs that inversely correlated with *Nf1* expression levels in brain samples (Hawes and Reilly, unpublished data). Given that *Nf1* levels do not show the same correlation to susceptibility in the peripheral nerve, it is unlikely that compensating overexpression of RasGEFs can account for differences in tumor susceptibility in all cell types. Furthermore, as lower levels of *Nf1* expression were similarly seen in the sciatic nerve of 129 mice, this could simply reflect an overall decrease in *Nf1* expression in the 129 background, irrespective of astrocytoma susceptibility.

In the sciatic nerve, a similar relationship of *Nf1* level to strain background was found in B6, 129, B6×A, and DBA as seen in the brain, suggesting that the control of *Nf1* expression can be globally modified in different strain backgrounds. In contrast, the expression level of *Nf1* in the B×D strains is higher than B6 levels in the sciatic nerve, unlike in the brain. This suggests that there may be additional tissue-specific modifiers of *Nf1* expression levels.

The most significant observation in this study is that the amount of decreased expression seen in haploinsufficient animals is as great as the magnitude of difference in *Nf1* expression levels between WT animals from different backgrounds. These data suggest that strain background has as much effect on *Nf1* expression as haploinsufficiency. Given that haploinsufficiency of *Nf1* is enough to alter biological processes, crossing different background strains with different *Nf1* expression levels, such as B6 and 129, may significantly affect the levels of *Nf1* expression in resultant progeny and potentially confound experimental conclusions. As an example (see Fig. 5), comparing the phenotype of WT mice carrying 129 modifiers of *Nf1* expression to *NPcis* mice carrying B6 modifiers of *Nf1* expression could potentially mask a true haploinsufficiency effect of *Nf1* mutation. On the other hand, comparing the phenotype of WT mice carrying B6 modifiers of *Nf1* expression to *NPcis* mice carrying 129 modifiers of *Nf1* expression could amplify the observed effect of *Nf1* haploinsufficiency on the phenotype. It is therefore important to examine haploinsufficient effects on well-defined inbred strain backgrounds rather than mixed backgrounds, particularly when crossing in interacting mutations that may be carried on a slightly different background.

Acknowledgment

This research was supported by the Intramural Research Program of the NIH, NCI. J.J.H. was supported by a grant from the National Academies. Special thanks to R. Williams for donation of the recombinant inbred B×D38, B×D39, and B×D40 mouse strains. Special thanks to K. Fox for animal care assistance and K. Cichowski for helpful discussions. GeneNetwork and WebQTL are supported by grant NIH P20-MH 62009. The INIA dataset was

generated with support from NIAAA-INIA to R. Williams. The HBP/Rosen Striatum dataset was generated with support from the NIH Human Brain Project (P20-DA 21131) to G. Rosen and R. Williams. All experiments were conducted in compliance with the current laws of the USA.

References

1. Pollack IF, Shultz B, Mulvihill JJ (1996) The management of brainstem gliomas in patients with neurofibromatosis 1. Neurology 46(6):1652–1660 [PubMed: 8649565]
2. Tonsgard JH (2006) Clinical manifestations and management of neurofibromatosis type 1. Semin Pediatr Neurol 13(1):2–7 [PubMed: 16818170]
3. Yohay K (2006) Neurofibromatosis types 1 and 2. Neurologist 12 (2):86–93 [PubMed: 16534445]
4. Ballester R et al. (1990) The NF1 locus encodes a protein functionally related to mammalian GAP and yeast IRA proteins. Cell 63(4):851–859 [PubMed: 2121371]
5. Martin GA et al. (1990) The GAP-related domain of the neurofibromatosis type 1 gene product interacts with ras p21. Cell 63(4):843–849 [PubMed: 2121370]
6. Xu GF et al. (1990) The neurofibromatosis type 1 gene encodes a protein related to GAP. Cell 62(3): 599–608 [PubMed: 2116237]
7. Xu GF et al. (1990) The catalytic domain of the neurofibromatosis type 1 gene product stimulates ras GTPase and complements ira mutants of *S. cerevisiae*. Cell 63(4):835–841 [PubMed: 2121369]
8. Ingram DA et al. (2000) Genetic and biochemical evidence that haploinsufficiency of the *Nf1* tumor suppressor gene modulates melanocyte and mast cell fates in vivo. J Exp Med 191(1):181–188 [PubMed: 10620616]
9. Kemkemer R et al. (2002) Increased noise as an effect of haploinsufficiency of the tumor-suppressor gene neurofibromatosis type 1 in vitro. Proc Natl Acad Sci USA 99(21):13783–13788 [PubMed: 12368469]
10. McLaughlin ME, Jacks T (2002) Thinking beyond the tumor cell: *Nf1* haploinsufficiency in the tumor environment. Cancer Cell 1 (5):408–410 [PubMed: 12124168]
11. Wu M, Wallace MR, Muir D (2006) *Nf1* haploinsufficiency augments angiogenesis. Oncogene 25(16):2297–2303 [PubMed: 16288202]
12. Yang FC et al. (2006) *Nf1* +/− mast cells induce neurofibroma like phenotypes through secreted TGF-{beta} signaling. Hum Mol Genet 15(16):2421–2437 [PubMed: 16835260]
13. Yu X et al. (2006) Neurofibromatosis type 1 gene haploinsufficiency reduces AP-1 gene expression without abrogating the anabolic effect of parathyroid hormone. Calcif Tissue Int 78(3):162–170 [PubMed: 16525748]
14. Atit RP et al. (1999) The *Nf1* tumor suppressor regulates mouse skin wound healing, fibroblast proliferation, and collagen deposited by fibroblasts. J Invest Dermatol 112(6):835–842 [PubMed: 10383727]
15. Jacks T et al. (1994) Tumour predisposition in mice heterozygous for a targeted mutation in *Nf1*. Nat Genet 7(3):353–361 [PubMed: 7920653]
16. Zhu Y et al. (2005) Inactivation of *NF1* in CNS causes increased glial progenitor proliferation and optic glioma formation. Development 132(24):5577–5588 [PubMed: 16314489]
17. Bennett MR et al. (2003) Aberrant growth and differentiation of oligodendrocyte progenitors in neurofibromatosis type 1 mutants. J Neurosci 23(18):7207–7217 [PubMed: 12904481]
18. Dasgupta B, Gutmann DH (2005) Neurofibromin regulates neural stem cell proliferation, survival, and astroglial differentiation in vitro and in vivo. J Neurosci 25(23):5584–5594 [PubMed: 15944386]
19. Powers J et al. (2000) Pheochromocytoma cell lines from heterozygous neurofibromatosis knockout mice. Cell Tissue Res 302(3):309–320 [PubMed: 11151443]
20. Tischler AS et al. (1995) Characterization of pheochromocytomas in a mouse strain with a targeted disruptive mutation of the neurofibromatosis gene *Nf1*. Endocr Pathol 6(4):323–335 [PubMed: 12114814]
21. Gutmann DH et al. (2001) Heterozygosity for the neurofibromatosis 1 (*NF1*) tumor suppressor results in abnormalities in cell attachment, spreading and motility in astrocytes. Hum Mol Genet 10(26):3009–3016 [PubMed: 11751683]

22. Bajenaru ML et al. (2001) Neurofibromatosis 1 (*NF1*) heterozygosity results in a cell-autonomous growth advantage for astrocytes. Glia 33(4):314–323 [PubMed: 11246230]
23. Chesler EJ et al. (2005) Complex trait analysis of gene expression uncovers polygenic and pleiotropic networks that modulate nervous system function. Nat Genet 37(3):233–242 [PubMed: 15711545]
24. Cichowski K et al. (1999) Mouse models of tumor development in neurofibromatosis type 1. Science 286(5447):2172–2176 [PubMed: 10591652]
25. Reilly KM et al. (2000) *Nf1*; Trp53 mutant mice develop glioblastoma with evidence of strain-specific effects. Nat Genet 26(1):109–113 [PubMed: 10973261]
26. Reilly KM et al. (2004) Susceptibility to astrocytoma in mice mutant for *Nf1* and Trp53 is linked to chromosome 11 and subject to epigenetic effects. Proc Natl Acad Sci USA 101(35):13008–13013 [PubMed: 15319471]
27. Vogel KS et al. (1999) Mouse tumor model for neurofibromatosis type 1. Science 286(5447):2176–2179 [PubMed: 10591653]
28. Reilly KM et al. (2006) An imprinted locus epistatically influences Nstr1 and Nstr2 to control resistance to nerve sheath tumors in a neurofibromatosis type 1 mouse model. Cancer Res 66(1): 62–68 [PubMed: 16397217]
29. Geist RT, Gutmann DH (1996) Expression of a developmentally-regulated neuron-specific isoform of the neurofibromatosis 1 (*NF1*) gene. Neurosci Lett 211(2):85–88 [PubMed: 8830850]
30. Hawes JJ et al. (2005) GalR1, but not GalR2 or GalR3, levels are regulated by galanin signaling in the locus coeruleus through a cyclic AMP-dependent mechanism. J Neurochem 93(5):1168–1176 [PubMed: 15934937]
31. Motulsky H (2003) Prism 4 Statistics Guide—statistical analyses for laboratory and clinical researchers. GraphPad Software, San Diego, CA
32. Park VM et al. (1998) Alternative splicing of exons 29 and 30 in the neurofibromatosis type 1 gene. Hum Genet 103(4):382–385 [PubMed: 9856477]
33. Vandenbroucke I et al. (2002) Quantification of *NF1* transcripts reveals novel highly expressed splice variants. FEBS Lett 522 (1–3):71–76 [PubMed: 12095621]

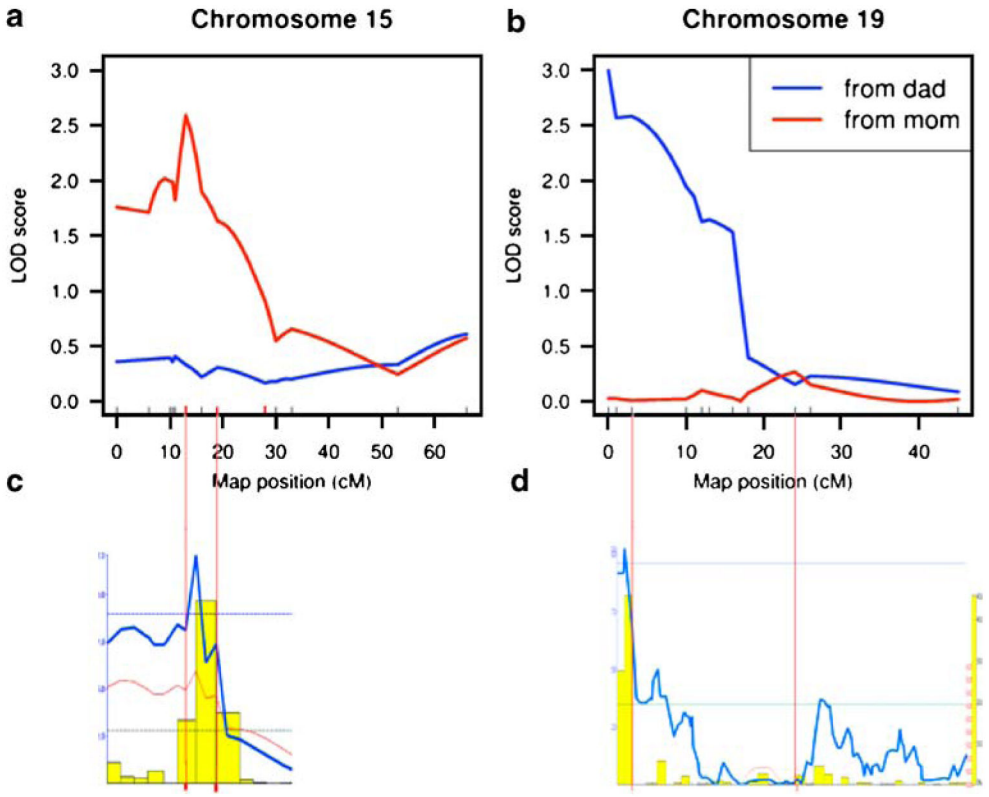

Fig. 1.

Comparison of nerve sheath tumor resistance loci, *Nstr1* and *Nstr2*, to quantitative trait loci for variation in *Nf1* expression levels. *Top panels* show previously identified *Nstr2* (**a**) on chromosome 15 and *Nstr1* (**b**) on chromosome 19 [28]. *Bottom panels* show interval mapping for levels of *Nf1* expression (Affy probe 1452525_a_at) in the striatum (**c**) and the mid- and forebrain (**d**). *Nstr1* and *Nstr2* linkage is dependent on whether *NPcis* mutant progeny are generated from mutant mothers (*red line*, **a** and **b**) or mutant fathers (*blue line*, **a** and **b**) [28]. In the *lower panels*, the likelihood ratio statistic (*LRS*) is shown in *blue*, and the additive effect is shown in *red*. The *horizontal dashed blue line* indicates statistically significant linkage based on permutation testing (genome-wide P=0.05), and the *horizontal dashed green line* indicates statistically suggestive linkage based on permutation testing (genome-wide P=0.63). *Yellow bars* indicate the frequency of the LRS peak location using bootstrap resampling. *Red vertical lines* between the *top* and *bottom panels* indicate common markers used in the two mapping studies and were used to calibrate the results of the WebQTL analysis to the results of the tumor susceptibility mapping

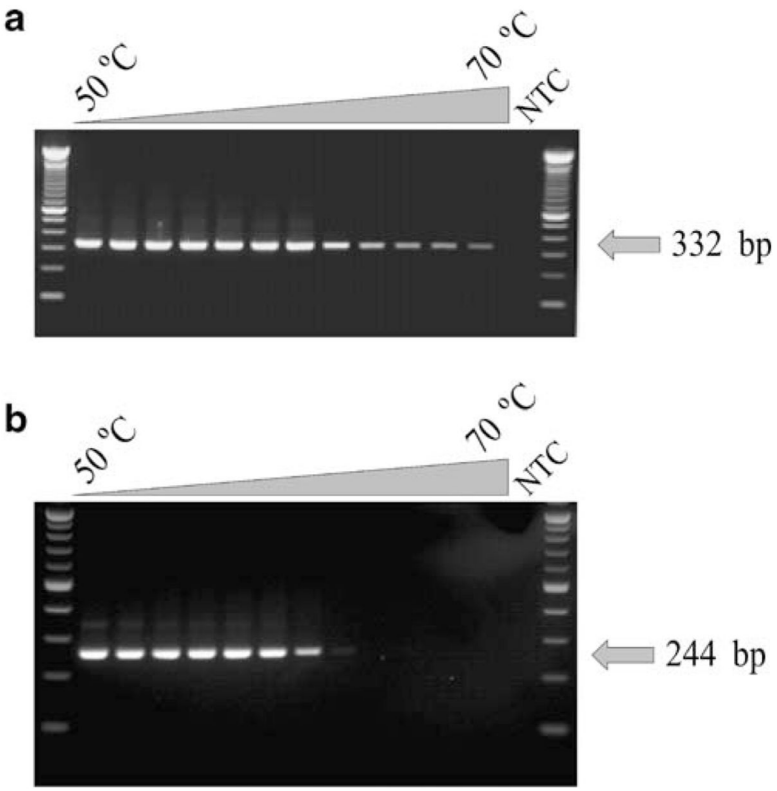

Fig. 2.

Standard PCR annealing temperature gradients from 50 to 70°C using *Nf1* primer set number 1 (**a**) and *Nf1* primer set number 2 (**b**). *Arrows* indicate the size of *Nf1* PCR products. *NTC* No template control

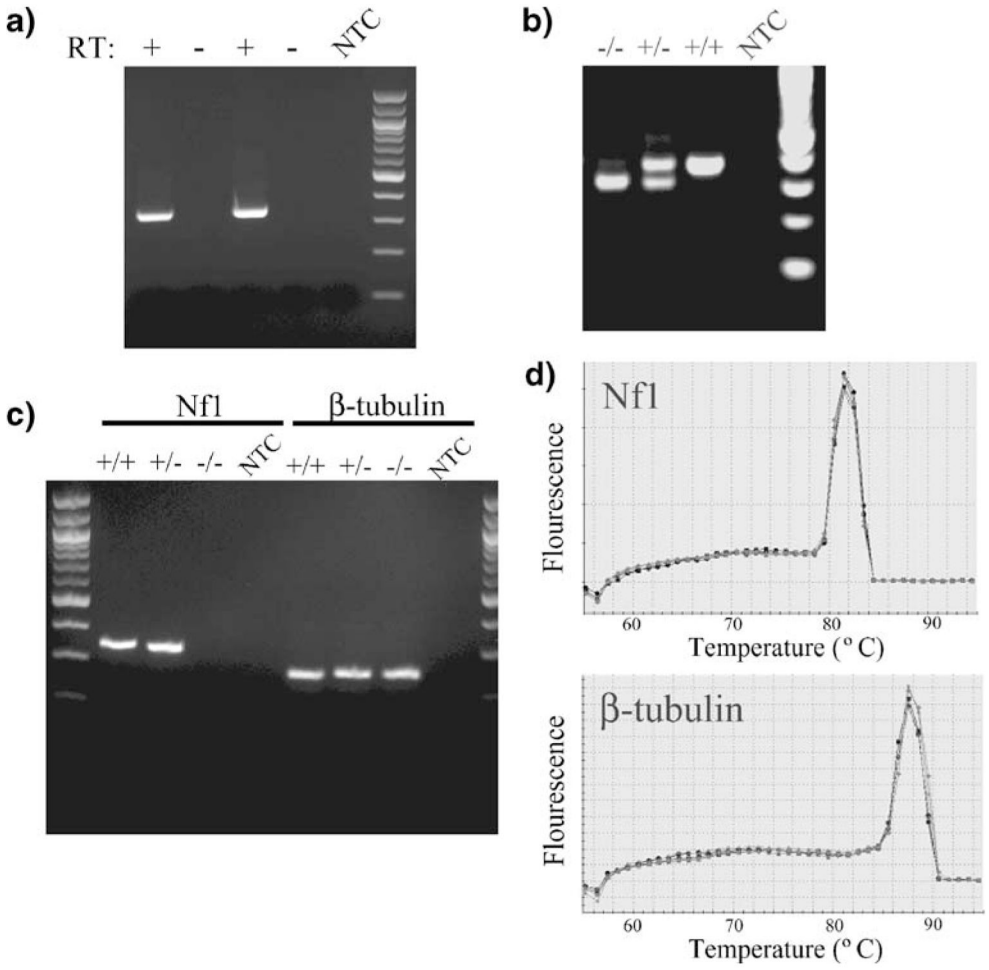

Fig. 3.

Nf1 qPCR primer controls ensure that the primers are specific for *Nf1* transcription. PCR product is only present in cDNA templates made in the presence of reverse transcriptase (+ RT) but not in templates containing only genomic DNA (− RT), (**a**). Genotyping of *Nf1* knockout (−/−) embryos isolated at E13.5 (**b**). *Nf1* and β-tubulin (internal control) PCR products using cDNA templates made from *Nf1* wild type (+/+), heterozygote (+/−), or knockout (−/−) embryos (**c**) reveal that *Nf1* product is absent in −/− templates. Single peaks in dissociation curves from *Nf1* and β-tubulin qPCR reactions indicate formation of a single product (**d**). *NTC* No template control

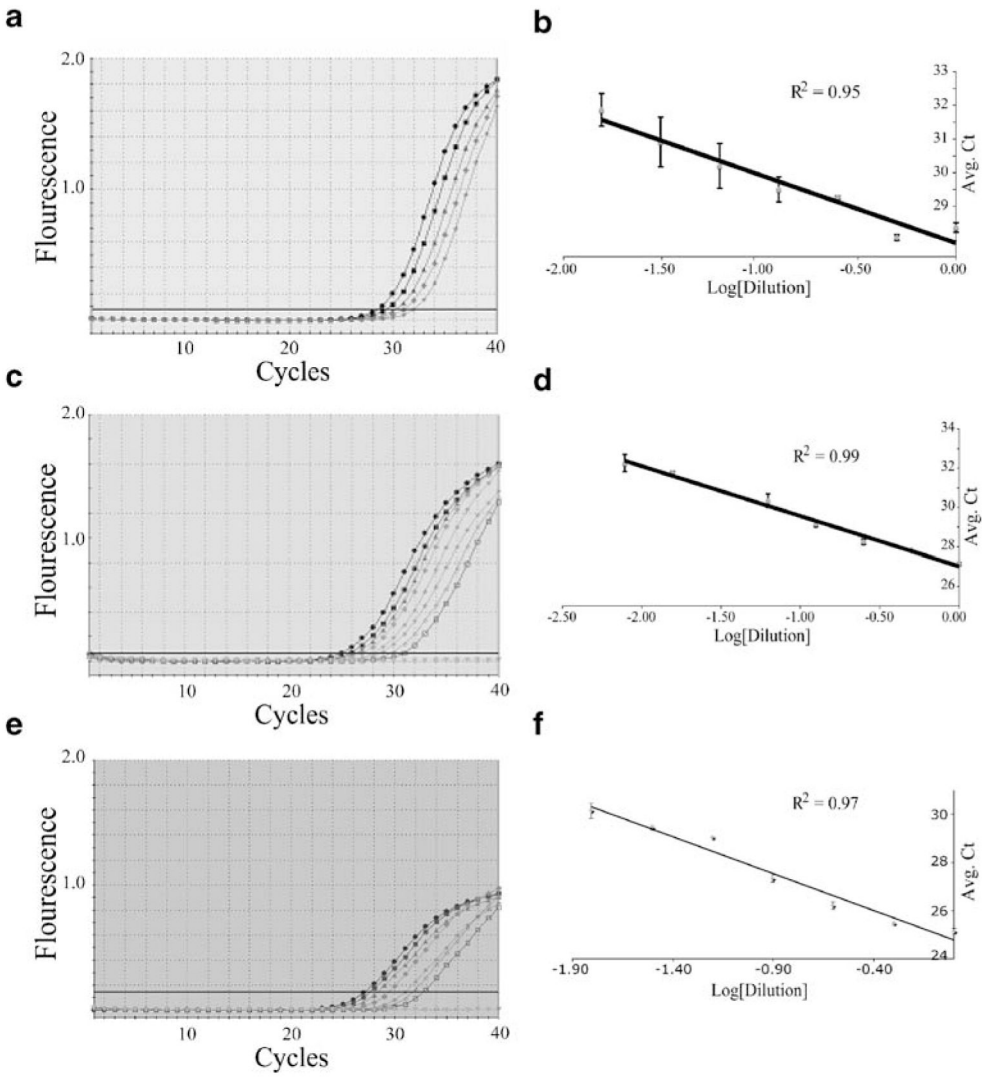

Fig. 4.

Nf1 qPCR product formation in reactions using *Nf1* primer set number 1 (**a, b**), *Nf1* primer set number 2 (**c, d**), and *Nf1* exon 9a primer set number 1 (**e, f**) is linear with respect to sequential template dilution. **a, c, e** Annealing temperature curves of the number of cycles required for product formation to reach threshold (Ct). **b, d, f** Determination of linearity regression values (R^2) for the formation of product versus serial dilution

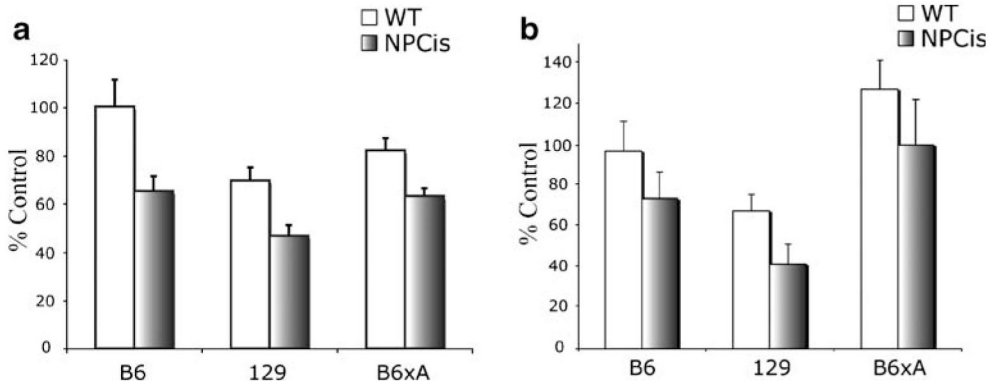

Fig. 5.

qPCR of *Nf1* (**a**) and *Nf1* exon 9a (**b**) expression levels in *NPcis* mice heterozygous for *Nf1* as compared to wild type (WT) animals on the same background strain. C57BL/6 (*B6*) WT *n*=6 and *NPcis n* = 5. 129S4/SvJae (*129*) WT *n*=7 and *NPcis n*=6. F1 progeny of C57BL/6 mice crossed with AJ mice (*B6×A*) WT *n*=5 and *NPcis n*=4)

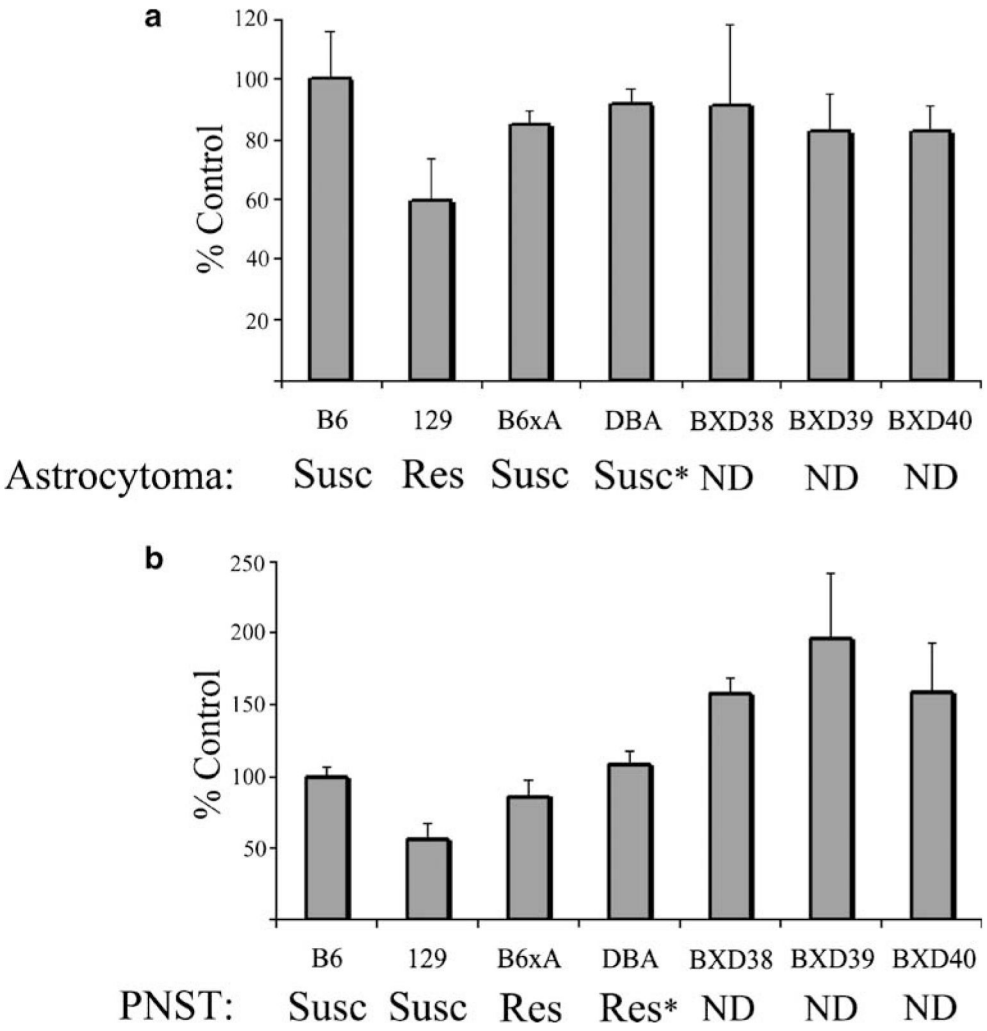

Fig. 6.

qPCR of *Nf1* expression levels in the brains of astrocytoma susceptible (*susc*) and resistant (*res*) background strains (**a**). *Nf1* expression levels in the sciatic nerve of background strains resistant or susceptible to peripheral nerve sheath tumors (GEM PNST; **b**). C57BL/6 (B6, *n*=4), 129S4/SvJae (129, *n*=4), F1 progeny of C57BL/6 mice crossed with AJ mice (B6×A, *n*=4) and DBA/2J (DBA, *n*=4), B×D38/TyJ (B×D38, *n*=2), B×D39/TyJ (B×D39, *n*=2), and B×D40/TyJ (B×D40, *n*=2). Susceptibility or resistance (*asterisk*) determined in F1 *NPCis*-B6×DBA mice ([26], unpublished data)